



Inclusive Searches for Squarks and Gluinos with the ATLAS detector

Jovan Mitrevski, on behalf of the ATLAS Collaboration

Fakultät für Physik, Ludwig-Maximilians-Universität München, München, Germany

Abstract

Despite the absence of experimental evidence, weak scale supersymmetry is one of the best motivated and studied Standard Model extensions. This paper summarises recent results on inclusive searches for supersymmetric squarks and gluinos obtained with the ATLAS detector at the LHC. Results are presented for searches in final state events containing jets, missing transverse momentum, leptons, or photons.

Keywords: ATLAS, LHC, SUSY

1. Introduction

Supersymmetry (SUSY) is an extension to the Standard Model (SM) that introduces a symmetry between fermions and bosons. In the Minimal Supersymmetric Standard Model (MSSM) there is a superpartner for each SM particle differing by 1/2 in spin but with otherwise identical quantum numbers. The symmetry is broken, however, because the superpartners do not have the same mass. If the SUSY particle masses are at the weak scale, SUSY solves the hierarchy problem and it may provide a dark matter candidate. Thus, weak scale SUSY remains one of the best motivated and studied SM extensions.

In minimal super-gravity-mediated SUSY breaking (MSUGRA/CMSSM) models, gravity-strength interactions are responsible for breaking supersymmetry. In gauge-mediated SUSY breaking (GMSB) models, the SUSY breaking is propagated to the MSSM sector via the standard gauge interactions. General Gauge Mediation (GGM) [1] is an effort to formulate gauge mediation in a general approach.

At the LHC, the production cross section to squarks (\tilde{q}) and gluinos (\tilde{g}), the superpartners of quarks and gluons respectively, tends to be the highest if they are not

too heavy. If R -parity is conserved, SUSY particles are produced in pairs, and the lightest SUSY particle (LSP) is stable. If the LSP does not interact appreciably with matter, it escapes the detector and is observed as missing transverse momentum (E_T^{miss} , and its magnitude E_T^{miss}). In MSUGRA models the LSP is often the lightest neutralino ($\tilde{\chi}_1^0$), while in GMSB models the LSP is the gravitino (\tilde{G}). In the latter case, the next to lightest SUSY particle (NLSP) determines the event signature.

After briefly describing the ATLAS detector in the next section, this paper presents recent ATLAS results on inclusive searches for squarks and gluinos in signatures consisting of jets and E_T^{miss} [2]; at least three b -jets and E_T^{miss} [3]; jets, at least one tau lepton, and E_T^{miss} [4]; two photons and E_T^{miss} [5]; and jet and two same-sign leptons or three leptons [6]. The analyses use 20.1–20.3 fb⁻¹ of data at a center-of-mass energy of 8 TeV.

2. ATLAS Detector

The ATLAS detector [7] is a multi-purpose apparatus with a forward-backward symmetric cylindrical geometry and nearly 4π solid angle coverage. Closest to the beamline is the inner detector, consisting of pixel and microstrip trackers covering $|\eta| < 2.5$ ¹ and a transition

Email address: Jovan.Mitrevski@cern.ch (Jovan Mitrevski)

¹ATLAS uses a right-handed coordinate system with its origin at the nominal interaction point (IP) in the centre of the detector and

radiation tracker covering $|\eta| < 2.0$. The inner detector is located inside a thin superconducting solenoid that provides a 2 T magnetic field.

Outside the solenoid, a fine-granularity lead/liquid-argon (LAr) electromagnetic (EM) calorimeter measures the energy and position of electrons and photons in the region $|\eta| < 3.2$. A presampler, covering $|\eta| < 1.8$, is used to correct for energy lost by particles before entering the EM calorimeter.

An iron/scintillating-tile hadronic calorimeter covers the region $|\eta| < 1.7$, while a LAr hadronic end-cap calorimeter covers $1.5 < |\eta| < 3.2$. In the forward region, $3.2 < |\eta| < 4.9$, LAr calorimeters with copper and tungsten absorbers measure both the electromagnetic and hadronic energy. A muon spectrometer, consisting of three superconducting toroidal magnet systems each comprising eight toroidal coils, tracking chambers, and detectors for triggering, surrounds the calorimeter system.

3. Object Definitions

The analyses used jets reconstructed using an anti- k_T algorithm with a radius parameter of 0.4 [8]. A neural-network-based algorithm was used for b -tagging [9] where needed. Electrons were reconstructed using clusters in the EM calorimeter matched to tracks [10], while photons were reconstructed from similar clusters not matched to tracks, or matched to tracks coming from a conversion vertex [11]. Muons were reconstructed from inner detector tracks matched to one or more segments in the muon spectrometer [12]. In the analysis with taus, hadronic taus were reconstructed from jets combining discriminating variables in a boosted decision tree (BDT) discriminator [13] and requiring one or three tracks. The E_T^{miss} was calculated using the transverse momenta of the reconstructed electrons, muons, jets, in the photon analysis photons, and calorimeter clusters not in those objects [14]. Taus were not separated from jets in the E_T^{miss} calculation.

Events were vetoed if they contained jets that fail certain quality selection criteria designed to suppress detector noise and non-collision backgrounds. This criteria tends to reject events with high- p_T photons, so other than in the dedicated analysis, event with photons were generally rejected.

the z -axis along the beam pipe. The x -axis points from the IP to the centre of the LHC ring, and the y -axis points upward. Cylindrical coordinates (r, ϕ) are used in the transverse plane, ϕ being the azimuthal angle around the beam pipe. The pseudorapidity is defined in terms of the polar angle θ as $\eta = -\ln \tan(\theta/2)$.

4. Analyses overview

The analyses defined signal regions (SRs) where to look for new physics, with different SRs optimized for different possible Beyond the Standard Model (BSM) scenarios. The analyses extracted both model-independent results and interpretations in various models using the CL_S prescription [15]. Control regions (CRs) were used to estimate some backgrounds, and validation regions (VRs) were used to validate the background modeling.

In addition to the object selection and kinematic cuts, the following variables were often used to define the signal, control, and validation regions. The transverse mass is defined as $m_T = \sqrt{2p_T^\ell E_T^{\text{miss}} (1 - \cos \Delta\phi_{\ell, E_T^{\text{miss}}})}$, where p_T^ℓ refers to the transverse momentum of a lepton. Events where the E_T^{miss} comes solely from the neutrino from a leptonic W boson decay have an end-point in this variable. The variable, H_T is usually defined as the scalar sum of all analysis-level jet, leptons, and photons, though some variations were used in some analyses. The variable, $m_{\text{eff}} = H_T + E_T^{\text{miss}}$ represents the *effective mass* of the system.

5. Search with Jets and E_T^{miss}

The search for squarks and gluinos in final states with jets and E_T^{miss} [2] is a very general search for BSM physics, with the main motivation being the pair production of squarks and gluinos ($\tilde{g}\tilde{g}$, $\tilde{q}\tilde{q}$, $\tilde{q}\tilde{g}$) in SUSY with R -parity conservation, where the LSP is a weakly-interacting neutralino ($\tilde{\chi}_1^0$). The analysis was optimized for various gluino and squark masses.

The analysis data were collected with a trigger requiring one jet and E_T^{miss} . All SRs required $E_T^{\text{miss}} > 160$ GeV and a leading jet with $p_T > 130$ GeV, so the trigger was fully efficient. Fifteen SRs were defined requiring a minimum of two to six jets, usually with $p_T > 60$ GeV. (Events with more jets were studied in a separate analysis [16].) Lower jet multiplicity SRs targeted squark pair production, while high multiplicity SRs targeted gluino production or long decay chains. There were multiple SRs with two, four, and six jets defined with various tightnesses, and there were two SRs, called 2jW and 4jW, specifically designed to target events with W bosons in the decay chains. The 2jW SR required that the event have two boosted W -jets, individual jets with $60 \text{ GeV} < m_{\text{inv}} < 100 \text{ GeV}$, while the 4jW SR required that there be at least one boosted W -jet and one resolved W candidate composed of two jets. Other selection criteria involved cuts on $\Delta\phi(\text{jet}, E_T^{\text{miss}})$, m_{eff} , and

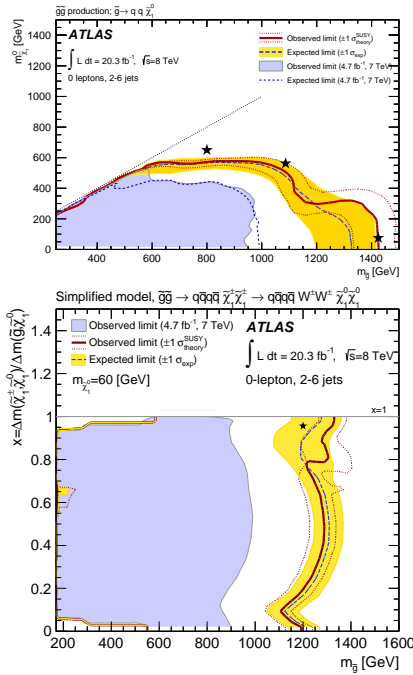


Figure 1: Exclusion limits for direct production of gluino pairs in simplified models where other particles are decoupled and the decays are to quarks and $\tilde{\chi}_1^0$ s or with W bosons [2]. The stars indicate benchmark models.

$E_T^{\text{miss}} / \sqrt{H_T}$ or $E_T^{\text{miss}} / m_{\text{eff}}$. The analysis vetoed events with any baseline electrons or photons to remain orthogonal to analyses requiring leptons.

The main backgrounds were Z + jets, W + jets, $t\bar{t}$, single top, and multi-jets. Z + jets was modeled with a γ + jets sample. W + jets and top backgrounds were normalized in control regions having a lepton, m_T consistent with the lepton coming from a W boson, and zero or at least one b -tagged jets, respectively. The multi-jet background was modeled using the jet smearing method [17].

No excess was seen, so limits were extracted. Model-independent limits were made in each SR, and the results were interpreted in various models, of which only a few examples are given below. Figure 1 gives the limits in simplified $\tilde{g}\tilde{g}$ models where the decays are as given in the figure. Limits for MSUGRA/CMSSM models are given in Sec. 10.

6. Search with at Least Three b -Jets and E_T^{miss}

The search for at least three b -jets and E_T^{miss} [3] targeted models with top or bottom quarks in the gluino decay chain or direct sbottom (\tilde{b} , the superpartner of a

bottom quark) production. These models are motivated by naturalness [18, 19], which prefers light stops (\tilde{t} , the superpartner of a top quark), at least one light \tilde{b} , and a relatively light \tilde{g} . More specifically, in addition to direct $\tilde{b}\tilde{b}$ pair production, $\tilde{g}\tilde{g}$ pair production with $\tilde{g} \rightarrow \tilde{b}_1 b$ or $\tilde{g} \rightarrow \tilde{t}_1 t$ was studied. The cases where the \tilde{b}_1 or \tilde{t}_1 is more massive than the \tilde{g} were also studied, and these models are known as Gbb, where $\tilde{g} \rightarrow b\tilde{b}\tilde{\chi}_1^0$, Gtt, where $\tilde{g} \rightarrow t\tilde{t}\tilde{\chi}_1^0$, and Gtb, where $\tilde{g} \rightarrow t b\tilde{\chi}_1^\pm$ and $\tilde{\chi}_1^\pm \rightarrow \tilde{\chi}_1^0 f f'$, with the mass difference being set so that f and f' do not contribute to the event selection.

The analysis used events that pass a E_T^{miss} trigger, which is greater than 99% efficient for the baseline selection of $E_T^{\text{miss}} > 150$ GeV and at least four jets with $p_T > 30$ GeV, the leading with $p_T > 90$ GeV, at least three of which must be b -tagged. The analysis was divided into two independent channels, the 1-lepton channel that had at least one electron or muon with $p_T > 25$ GeV, and the 0-lepton channel that did not. In the 1-lepton channel, three SRs were defined requiring at least six jets and different E_T^{miss} , m_T , and m_{eff} selections. In the 0-lepton channel, three SRs were defined requiring at least four jets and three requiring at least seven jets. The jet p_T , E_T^{miss} , m_{eff} , and $E_T^{\text{miss}} / \sqrt{H_T}$ cuts differed between the SRs, and one 4-jet SR required the leading jet to not be b -tagged in order to select events recoiling against ISR to target low mass splitting scenarios. The 0-lepton SRs also made requirements on $\Delta\phi(\text{jet}, \mathbf{E}_T^{\text{miss}})$, and $E_T^{\text{miss}} / m_{\text{eff}}$. The 4-jet 0-lepton channels targeted events with sbottoms, while the 1-lepton and 7-jet 0-lepton SRs targeted events with stops.

The background was dominated by $t\bar{t}$ +jets events. The $t\bar{t}$ +jets background with fake b -jets was estimated with matrix method based on the probabilities to b -tag and mistag different types of jets, while the background with all real b -jets was estimated by a fit to a CR with a two lepton requirement, reduced E_T^{miss} requirement, and reversed m_T . Minor backgrounds were modeled using MC events.

No excess was seen. Model-independent limits were made in each SR, and the results were interpreted in various models, of which only a few examples are given below. Figure 2 gives the limits in simplified $\tilde{g}\tilde{g}$ models decaying to on-shell stops and in the Gtb models. Limits for the Gtt models are given in Sec. 10.

7. Search with Jets, At Least One Tau Lepton, and E_T^{miss}

The search for jets, at least one tau lepton, and E_T^{miss} [4] targeted GMSB, both minimal and natural

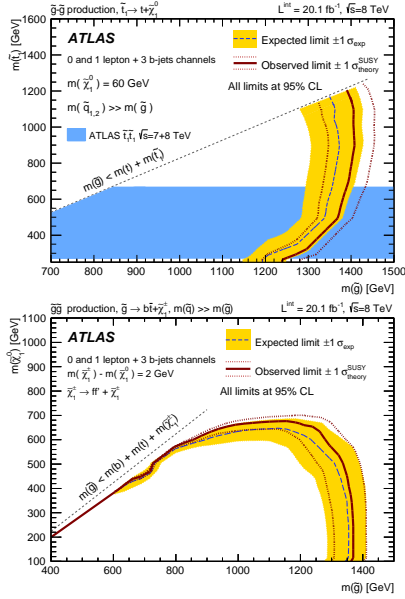


Figure 2: Exclusion limits for direct production of gluino pairs in simplified models where the gluinos decay to on-shell stops and in the Gtb model [3].

gauge mediation (nGM, based on the GGM framework) [20], MSUGRA/CMSSM, and bilinear R -parity violating (bRPV) models [21]. Minimal and general GMSB models can have a stau ($\tilde{\tau}$, the superpartner of the tau) NLSP, potentially close in mass with selectrons and smuons, the superpartners of electrons and muons.

Four topologies were studied: (1τ) exactly one tau with $p_T > 30$ GeV, (2τ) two or more taus with $p_T > 20$ GeV, and ($\tau + e/\mu$) one or more taus ($p_T > 20$ GeV) and one exactly one e/μ . The 1τ and 2τ topologies were triggered with a jet+ E_T^{miss} trigger while the $\tau + e/\mu$ analyses instead were triggered by a single lepton trigger.

A number of SRs were created in the various topologies, making additional cuts on E_T^{miss} , m_T , H_T , m_{eff} , and $\Delta\phi(\text{jet}, \mathbf{E}_T^{\text{miss}})$. The 1τ topology had a tight and a loose SR, the latter for more model independent searches. The 2τ topology had four SRs, three targeting minimal GMSB, nGM, and bRPV models separately, and the fourth for more model independent searches. The $\tau + e/\mu$ topologies each had four SRs, targeting GMSB, nGM, bRPV, and MSUGRA/CMSSM. Two of these SRs did not have any explicit E_T^{miss} requirements.

The main backgrounds were W +jets, Z +jets, top, and multi-jets. The first three were modeled by normalizing in control regions, while multi-jets were modeled differently in different channels. In the 1τ topology, multi-jets used the $ABCD$ method, defining four exclusive regions by varying tau identification tightness and a combina-

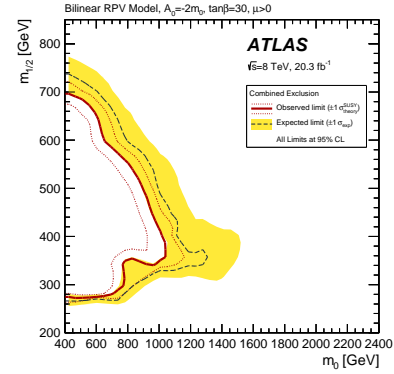


Figure 3: Exclusion limits in the bRPV model [4].

tion of E_T^{miss} and $\Delta\phi(\text{jet}, \mathbf{E}_T^{\text{miss}})$. The 2τ topology used the jet smearing method [17], and the $\tau + e/\mu$ topologies used a matrix method using the different isolation efficiencies of real and fake taus. Minor diboson backgrounds were modeled with MC.

No excess was seen. Model-independent limits were made in each SR, and the results were interpreted in the various models. In the minimal GMSB model with $M_{\text{mess}} = 250$ TeV, $N_5 = 3$, $\mu > 0$, and $C_{\text{grav}} = 1$, values of the SUSY breaking scale Λ below 63 TeV are excluded for all $\tan\beta$, and in the nGM model studied, gluinos below 1090 GeV were excluded. Figure 3 gives the limits in the bRPV models. Limits for MSUGRA/CMSSM models are given in Sec. 10.

8. Search with Two Photons and E_T^{miss}

The search for two photons and E_T^{miss} [5] was motivated by GMSB models with a bino-like $\tilde{\chi}_1^0$ NLSP. The GGM framework was used to define simplified models where all masses were high other than the $\tilde{\chi}_1^0$, the \tilde{G} , and either a gluino or a wino for strong or weak production, respectively. In this paper we focus only on the strong production mechanism: gluino pair production. The events were triggered by a diphoton trigger, which was almost fully efficient given the offline selection of at least two tight photons with $p_T > 75$ GeV. Cuts were applied on $\Delta\phi(\text{jet}, \mathbf{E}_T^{\text{miss}})$ and in some SRs $\Delta\phi(\gamma, \mathbf{E}_T^{\text{miss}})$ to decrease the background with fake E_T^{miss} . Two “strong” SRs were defined, cutting strongly on E_T^{miss} and m_{eff} , optimized separately for low-mass and high-mass NLSPs, two “weak” SRs were defined, cutting less strongly on E_T^{miss} and H_T , again optimized for low-mass and high-mass NLSPs, and one “model independent signal” (MIS) SR was defined, selecting only on E_T^{miss} , not on H_T or m_{eff} .

Backgrounds were modeled using control samples and CRs. The fake E_T^{miss} background was modeled with a *QCD control sample*, requiring one tight photon and one loose-but-not-tight photon while leaving the other SR cuts the same. Electrons were vetoed to decrease the $W + \text{jets}$ contamination. This sample was normalized to the low E_T^{miss} region for the weak and MIS SRs, but since the statistics were too low for the strong SRs, a variation was used, loosening the m_{eff} selection and extrapolating to high m_{eff} . The $W + X$ background, where X contains at most one photon, was modeled by using an electron-photon control sample, scaled by the electron to photon fake rate. The $W\gamma\gamma$ background used MC normalized to a CR for the background estimate, while the smaller $Z\gamma\gamma$ background was normalized to the calculated NLO cross section.

No excess was found. Model-independent limits were made, and in the model-dependent strong production model, gluinos were excluded with mass smaller than 1280 GeV for bino masses above 50 GeV.

9. Search with Jets and Two Same-Sign Leptons or Three Leptons

The search for SUSY in final states with jets and two same-sign leptons or three leptons [6] is a low-background search for BSM physics, with many interpretations. Because it has low background, it can use looser requirements and thus also target low E_T^{miss} scenarios, like R -parity violating (RPV) models and compressed spectra.

Because gluinos are Majorana particles, gluino pair production can lead to same-sign signatures. Both gluino and squark production can also lead to same-sign leptons or three leptons in the decay chain. This analysis targeted gluino-mediated top squark production, gluino-mediated (and direct) first and second generation squark production with W , Z , and slepton particles in the decays, and direct sbottom production with $\tilde{b} \rightarrow t\tilde{\chi}_1^\pm$.

Five independent signal regions were designed to cover these signatures, which were combined for increased sensitivity. These used either a same-sign sample (SS), defined to have two same-sign electrons or muons, the leading (second) with $p_T > 20(15)\text{ GeV}$ and no other electrons or muons with $p_T > 15\text{ GeV}$, or a three-lepton signature (3L), requiring at least three leptons with $p_T > [20, 15, 15]\text{ GeV}$. SRs that had b -tagged jet requirements targeted signals with stops and sbottoms, while other SRs targeted first and second generation squarks. Two SRs had either no or low E_T^{miss} requirements, useful for compressed and RPV scenarios.

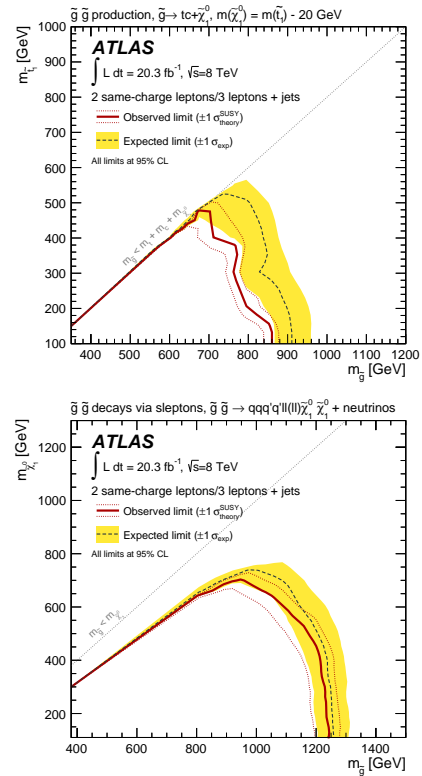


Figure 4: Exclusion limits in gluino-mediated stop and first and second generation squark production [6].

Other variables used to define the signal regions were N_{jets} , m_T , m_{eff} , and a Z boson veto.

The main backgrounds were prompt multilepton, fake leptons, and in the SS sample for electrons, charge mis-measurement. The prompt multilepton background was mainly from $t\bar{t}V$ and diboson events. These were modeled from MC samples normalized to NLO calculations. The fake lepton background was modeled using a matrix method. The charge mis-measurement probability for electrons was extracted from two Z boson control samples, one with opposite-sign electron pairs, one with same-sign electron pairs.

No significant excess was observed, but small excesses were seen in two SS signal regions with significances of 1.5 and 1.8 standard deviations respectively. Model-independent limits were made in each SR, and the results were interpreted in the various models, of which a few examples are given below in Fig. 4. Limits for the MSUGRA/CMSSM and Gtt models are given in Sec. 10.

Additional lepton-based inclusive SUSY searches not discussed were performed using 8 TeV data [22, 23].

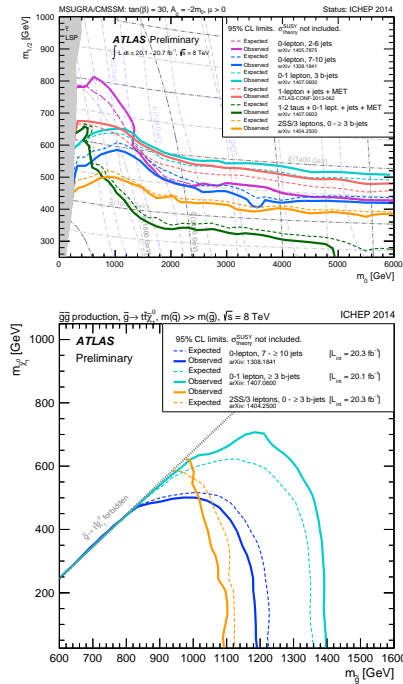


Figure 5: Exclusion limits in the MSUGRA and Gtt models overlaying the plots of multiple analyses.

10. Summary and Conclusion

Fig. 5 gives exclusion limits for MSUGRA/CMSSM models with the remaining parameters set to $\tan(\beta) = 30$, $A_0 = 2m_0$, $\mu > 0$ and for Gtt simplified models for the analyses presented in this paper. The ATLAS experiment is continuing to expand the reach of inclusive gluino and squark searches. Moreover, many BSM scenarios, both with and without SUSY, are covered by these searches. Nothing unexpected has been found yet; however, run 2 of LHC is expected to significantly expand this reach. At 13 TeV, the production cross section is tens of times greater for 1.5 TeV gluinos, and thousands of time greater at 2.5 TeV.

References

- [1] P. Meade, et al., General Gauge Mediation, Prog. Theor. Phys. Suppl. 177 (2009) 143–158.
- [2] ATLAS Collaboration, Search for squarks and gluinos with the ATLAS detector in final states with jets and missing transverse momentum using $\sqrt{s} = 8$ TeV proton–proton collision data, JHEP 1409 (2014) 176.
- [3] ATLAS Collaboration, Search for strong production of supersymmetric particles in final states with missing transverse momentum and at least three b -jets at $\sqrt{s} = 8$ TeV proton-proton collisions with the ATLAS detector, JHEP 1410 (2014) 24.

- [4] ATLAS Collaboration, Search for supersymmetry in events with large missing transverse momentum, jets, and at least one tau lepton in 20fb^{-1} of $\sqrt{s} = 8$ TeV proton-proton collision data with the ATLAS detector, JHEP 1409 (2014) 103.
- [5] ATLAS Collaboration, Search for diphoton events with large missing transverse momentum in 8 TeV pp collision data with the ATLAS detector, Tech. Rep. ATLAS-CONF-2014-001, CERN, Geneva (Jan 2014).
- [6] ATLAS Collaboration, Search for supersymmetry at $\sqrt{s} = 8$ TeV in final states with jets and two same-sign leptons or three leptons with the ATLAS detector, JHEP 1406 (2014) 035.
- [7] ATLAS Collaboration, The ATLAS Experiment at the CERN Large Hadron Collider, JINST 3 (2008) S08003.
- [8] M. Cacciari, et al., The Anti- k_T jet clustering algorithm, JHEP 0804 (2008) 063.
- [9] ATLAS Collaboration, Measurement of the b -tag efficiency in a sample of jets containing muons with 5fb^{-1} of data from the ATLAS detector, Tech. Rep. ATLAS-CONF-2012-043, CERN, Geneva (Mar 2012).
- [10] ATLAS Collaboration, Electron efficiency measurements with the ATLAS detector using the 2012 LHC proton-proton collision data, Tech. Rep. ATLAS-CONF-2014-032, CERN, Geneva (Jun 2014).
- [11] ATLAS Collaboration, Measurements of the photon identification efficiency with the ATLAS detector using 4.9fb^{-1} of pp collision data collected in 2011, Tech. Rep. ATLAS-CONF-2012-123, CERN, Geneva (Aug 2012).
- [12] ATLAS Collaboration, Measurement of the muon reconstruction performance of the ATLAS detector using 2011 and 2012 LHC proton-proton collision data, submitted to EPJC, arXiv:1407.3935.
- [13] ATLAS Collaboration, Identification of the hadronic decays of tau leptons in 2012 data with the ATLAS detector, Tech. Rep. ATLAS-CONF-2013-064, CERN, Geneva (Jul 2013).
- [14] ATLAS Collaboration, Performance of missing transverse momentum reconstruction in proton-proton collisions at $\sqrt{s} = 7$ TeV with ATLAS, Eur.Phys.J. C72 (2012) 1844.
- [15] A. L. Read, Presentation of search results: The CL_s technique, J.Phys.G G28 (2002) 2693.
- [16] ATLAS Collaboration, Search for new phenomena in final states with large jet multiplicities and missing transverse momentum at $\sqrt{s} = 8$ TeV proton-proton collisions using the ATLAS experiment, JHEP 1310 (2013) 130.
- [17] ATLAS Collaboration, Search for squarks and gluinos with the ATLAS detector in final states with jets and missing transverse momentum using 4.7fb^{-1} of $\sqrt{s} = 7$ TeV proton-proton collision data, Phys.Rev. D87 (2013) 012008.
- [18] R. Barbieri, G. Giudice, Upper bounds on supersymmetric particle masses, Nucl.Phys. B306 (1988) 63.
- [19] B. deCarlos, J. Casas, One loop analysis of the electroweak breaking in supersymmetric models and the fine tuning problem, Phys.Lett. B309 (1993) 320–328. arXiv:hep-ph/9303291.
- [20] J. Barnard, et al., Natural gauge mediation with a bino NLSP at the LHC, Phys.Rev.Lett. 109 (2012) 241801.
- [21] M. Hirsch, et al., Neutrino masses and mixings from supersymmetry with bilinear R -parity violation: A theory for solar and atmospheric neutrino oscillations, Phys.Rev. D62 (2000) 113008.
- [22] ATLAS Collaboration, Search for squarks and gluinos in events with isolated leptons, jets and missing transverse momentum at $\sqrt{s} = 8$ TeV with the ATLAS detector, Tech. Rep. ATLAS-CONF-2013-062, CERN, Geneva (Jun 2013).
- [23] ATLAS Collaboration, Search for strongly produced supersymmetric particles in decays with two leptons at $\sqrt{s} = 8$ TeV, Tech. Rep. ATLAS-CONF-2013-089, CERN, Geneva (Aug 2013).